Comp. Appl. Math.
DOI 10.1007/s40314-015-0234-3

Dynamics and bifurcations in a simple quasispecies model of tumorigenesis

Vanessa Castillo[1] · **J. Tomás Lázaro**[1] · **Josep Sardanyés**[2,3]

Received: 12 November 2014 / Revised: 20 March 2015 / Accepted: 22 April 2015

Abstract Cancer is a complex disease and thus is complicated to model. However, simple models that describe the main processes involved in tumoral dynamics, e.g., competition and mutation, can give us clues about cancer behavior, at least qualitatively, also allowing us to make predictions. Here, we analyze a simplified quasispecies mathematical model given by differential equations describing the time behavior of tumor cell populations with different levels of genomic instability. We find the equilibrium points, also characterizing their stability and bifurcations focusing on replication and mutation rates. We identify a transcritical bifurcation at increasing mutation rates of the tumor cells. Such a bifurcation involves a scenario with dominance of healthy cells and impairment of tumor populations. Finally, we characterize the transient times for this scenario, showing that a slight increase beyond the critical mutation rate may be enough to have a fast response towards the desired state (i.e., low tumor populations) by applying directed mutagenic therapies.

Keywords Applied mathematics · Bifurcations · Cancer · Complex systems · Quasispecies dynamics

Communicated by Maria do Rosario de Pinho.

✉ J. Tomás Lázaro
jose.tomas.lazaro@upc.edu

✉ Josep Sardanyés
josep.sardanes@upf.edu

[1] Department of Applied Mathematics, Universitat Politècnica de Catalunya, Avinguda Diagonal 647, 08028 Barcelona, Spain

[2] ICREA-Complex Systems Lab, Department of Experimental and Health Sciences, Universitat Pompeu Fabra, Parc de Recerca Biomèdica de Barcelona (PRBB), Dr. Aiguader 88, 08003 Barcelona, Spain

[3] Institut de Biologia Evolutiva (CSIC-Universitat Pompeu Fabra), Passeig Maritim de la Barceloneta 37, 08003 Barcelona, Spain

Published online: 15 May 2015

Mathematics Subject Classification 92Bxx Mathematical biology in general · 65Lxx ODEs · 58Kxx catastrophe theory · 37G35 Attractors and their bifurcations · 70K50 bifurcations and instability

1 Introduction

Cancer progression is commonly viewed as a cellular microevolutionary process (Cairns 1975; Merlo et al. 2006). Genomic instability, which seems to be a common trait in most types of cancer (Cahill et al. 1999), is a key factor responsible for tumor progression since it allows a Darwinian exploratory process required to overcome selection barriers. By displaying either high levels of mutation or chromosomal aberrations, cancer cells can generate a progeny of highly diverse phenotypes able to evade such barriers (Loeb 2001). Genomic instability refers to an increased tendency of alterations in the genome during the life cycle of cells. Normal cells display a very low rate of mutation (1.4×10^{-10} changes per nucleotide and replication cycle). Hence, it has been proposed that the spontaneous mutation rate in normal cells is not sufficient to account for the large number of mutations found in human cancers. Indeed, studies of mutation frequencies in microbial populations, in both experimentally induced stress and clinical cases, reveal that mutations that inactivate mismatch repair genes result in $10^2 - 10^3$ times the background mutation rate (Oliver et al. 2000; Bjedov et al. 2003; Sniegowski et al. 1997). Also, unstable tumors exhibiting the so-called mutator phenotype (Loeb 2001) have rates that are at least two orders of magnitude higher than in normal cells (Anderson et al. 2001; Bielas et al. 2006). This difference leads to cumulative mutations and increased levels of genetic change associated to further failures in genome maintenance mechanisms (Hoeijmakers 2001). The amount of instability is, however, limited by too high levels of instability, which have been suggested to exist in tumor progression (Cahill et al. 1999), thus indicating that thresholds for instability must exist. In fact, many anticancer therapies indirectly take advantage of increased genomic instability, as is the case of mitotic spindle alteration by taxol or DNA damage by radiation or by alkylating agents.

The mutator phenotype is the result of mutations in genes which are responsible of preserving genomic stability, e.g., breast cancer 1 (BRCA1), bloom syndrome protein (BLM), ataxia telangiectasia mutated (ATM) or gene protein P53 (which is involved in multitude of cellular pathways responsible of cell cycle control, DNA repair, among others). This mutator phenotype undergoes increases in mutation rates and can accelerate genetic evolution in cancer cells that can ultimately drive to tumor progression (Loeb 2001). As mentioned, genomic instability is a major driving force in tumorigenesis. Tumorigenesis can be viewed as a process of cellular microevolution in which individual preneoplastic or tumor cells acquire mutations that can increase proliferative capacity and thus confer a selective advantage in terms of growth speed. The rate of replication of tumor cells can increase due to mutations in both tumor suppressor genes, e.g., adenomatous polyposis coli (APC) or P53; and oncogenes, e.g., rat sarcoma (RAS) or SRC. Tumor suppressor genes protect cells from one step on the path to cancer and oncogenes are genes that, when mutated, have the potential to cause cancer. In terms of population dynamics, alterations in both types of genes drive to neoplastic process through increases in cancer cells numbers. Mutations in replication-related genes that confer an increase of fitness and thus a selective advantage are named driver mutations (Benedikt et al. 2014). This evolutionary process allows tumor cells to escape the restrictions that limit growth of normal cells, such as the constraints imposed by the immune system, adverse metabolic conditions or cell cycle checkpoints.

The iterative process of mutation and selection underlying tumor growth and evolution promotes the generation of a diverse pool of tumor cells carrying different mutations and chromosomal abnormalities. In this sense, it has been suggested that the high mutational capacity of tumor cells, together with an increase of proliferation rates, may generate a highly diverse population of tumor cells similar to a quasispecies (Solé 2001; Brumer et al. 2006). A quasispecies is a "cloud" of genetically related genomes around the so-called master sequence, which is at the mutation–selection equilibrium (Eigen 1971; Eigen and Schuster 1979). Due to the heterogeneous population structure, selection does not act on a single mutant but on the quasispecies as a whole. The most prominent examples of a quasispecies are given by RNA viruses [e.g. Hepatitis C virus (Solé et al. 2006), vesicular stomatitis virus (Marcus et al. 1998), the human immunodeficiency virus type 1 (Cichutek et al. 1992), among others].

An important concept in quasispecies theory is the so-called error threshold (Eigen 1971; Eigen and Schuster 1979). The error threshold is a phenomenon that involves the loss of information at high mutation rates. According to Eigen's original formulation, a quasispecies can remain at equilibrium despite high mutation rates, but the surpass of the critical mutation rate will upset this balance since the master sequence itself disappears and its genetic information is lost due to the accumulation of errors. It has been suggested that many RNA viruses replicate near the error threshold (Domingo et al. 2001). Another important concept in quasispecies theory is lethal mutagenesis. As a difference from the error threshold (which is a shift in sequence space), lethal mutagenesis is a process of demographic extinction due to an unbearable number of mutations (Bull et al. 2007; Wylie and Shakhnovich 2012). Most basically, it requires that deleterious mutations are happening often enough that the population cannot maintain itself, but it is otherwise no different from any other extinction process in which fitness is not great enough for one generation of individuals to fully replace themselves in the next generation. In simple words, increased mutagenesis could impair the maintenance of a quasispecies due to the crossing of the error threshold or due to lethal mutagenesis.

Quasispecies theory has provided a population-based framework for understanding RNA viral evolution (Lauring and Andino 2010). These viruses replicate at extremely high mutation rates and exhibit significant genetic diversity. This diversity allows a viral population to rapidly adapt to dynamic environments and evolve resistance to vaccines and antiviral drugs. As we previously mentioned, several features have been suggested to be shared between RNA viruses and tumors (Sardanyés et al. 2014), at least qualitatively. One is the presence of high levels of heterogeneity, both at genotype and phenotype levels. Typically, cancer cells suffer mutations affecting cell communication, growth and apoptosis (i.e., programmed cell death). Accordingly, escape from the immune system (and other selection barriers) operates in both RNA viruses and tumors. Viruses use antigenic diversity, whereas tumors evade the immune system by loosing their antigens through mutation, or making use of antigenic modulation and/or tumor-induced immune suppression. Even more, similar to RNA viruses, genetic instability in cancer cells will have detrimental effects on cells fitness, since most random mutations are likely to be harmful. As indicated by Cahill et al. (1999), the best chance of cure advanced cancers might be a result of tumor genetic instability: cancer cells are more sensitive to stress-inducing agents. In this sense, possible therapies increasing mutation of tumor cells could push this population towards the error threshold or induce lethal mutagenesis. This is the topic that we will address in this work using a mathematical model describing the dynamics of competition between different cell populations with different levels of genomic instability. Specifically, we will find equilibrium points, characterizing their stability, focusing on possible changes in the stability as a function of the mutation rate and the fitness of cell

populations. We will also investigate the transient times of the system to reach a given equilibrium state.

Each of the mathematical results will be given in terms of the mutation rates or the replication fidelity of the cells. This is important to understand how tumor populations behave. As we previously mentioned, unstable cells may reach an error threshold and start loosing genetic information until its population decreases or, even more, disappears. We will see how mutation rates affect this error threshold. Furthermore, we will see how they affect to the velocity of the tumor population to reach an equilibrium point, which is interesting since mutation rates can be manipulated and externally modified by means of mutagenic drugs [similar to RNA viruses (Crotty et al. 2001)] or radiotherapy.

2 The model

In this section, we introduce the model by Solé and Deisboeck (2004), which describes the competitive behavior between cell populations with different levels of genomic instability. The model is given by the following set of differential equations:

$$\begin{cases} \dot{x_0} = f_0 Q x_0 - \Phi(x_0, x_1, x_2)x_0, \\ \dot{x_1} = f_0(1-Q)x_0 + f_1 Q' x_1 - \Phi(x_0, x_1, x_2)x_1, \\ \dot{x_2^i} = f_1(1-Q')q_i' x_1 + \sum_{j=1}^{n} f_2^j \mu_{ij} x_2^j - \Phi(x_0, x_1, x_2)x_2^i. \end{cases} \tag{1}$$

The state variable x_0 is the fraction of cells with anomalous growth but no genetic instability; x_1 is the fraction of cells derived from x_0 by mutation that allows genetic instability; and x_2^i for $i = 1, 2 \ldots, n$ is the fraction of tumor mutant cells that can be generated from x_1 due to mutation (see Fig. 1). Thus, x_0, x_1 and x_2^i denote the fraction of each population and, therefore, the sum of all these variables must be exactly one, i.e., $x_0 + x_1 + \sum_{i=1}^{n} x_2^i = 1$. Moreover, the probability of mutation from x_1 to x_2^i can be denoted by $\mu_{x_1 \to x_2^i}$ and is given by $(1-Q')q_i'$. Notice that $\sum_{i=1}^{n} q_i' = 1$. Coefficients μ_{ij} denote the mutation rate (or probability) from x_2^j to x_2^i. The probability of error-free replication of x_2^i is represented by μ_{ii}. Additionally, cross-mutations connect the different subclones of x_2 through the term $\sum_{j=1}^{n} f_2^j \mu_{ij} x_2^j$, being f_j the growth rate of each population and f_2^i the growth rate of each subpopulation of x_2. These f_j and f_2^i are known as the fitness of each population. The greater is the fitness of

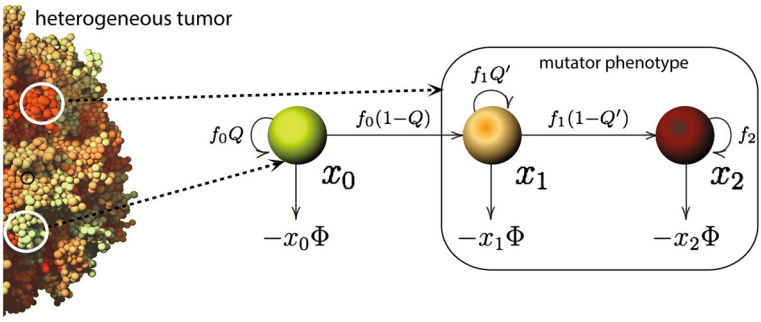

Fig. 1 Schematic diagram of the investigated system. We consider a simple model of tumor growth describing the dynamics of competition between different cell populations with different levels of genomic instability. Three different cell populations are considered: x_0 represents anomalous growth but low genomic instability, and both x_1 and x_2 have larger genomic instabilities (see Sect. 2 for a description of the model parameters)

a population, the greater is its replicative rate. Finally, the term $\Phi(\mathbf{x})$ is the average fitness of the population vector $\mathbf{x} = (x_0, x_1, x_2^1, x_2^2, \ldots, x_2^n)$, i.e., $\Phi(\mathbf{x}) = f_0 x_0 + f_1 x_1 + \sum_{i=1}^{n} f_2^i x_2^i$. $\Phi(\mathbf{x})$ is also known as the "constant population constraint" and it ensures that the population remains constant, also introducing competition all cell populations. Although the model does not explicitly consider environmental constraints, such as blood supply, hypoxia or acidosis, they can be considered as implicitly introduced through the set $\{f_j\}_{j=0,1,2}$ (Solé 2001). Population x_0 mutates to x_1 with a probability of $\mu_0 = 1 - Q$. In the same way, x_1 mutates in different x_2^i-sequences with a probability $\mu_1 = 1 - Q'$. In both cases, $0 < Q, Q' < 1$, being Q and Q' the copying fidelity during replication for x_0 and x_1, respectively. So, in this model, mutations from x_1 to x_0 and from x_2^i to x_1 have not been considered. It is also worth noticing that the model with $Q' = 1$ is the two-variable quasispecies model (Swetina and Schuster 1982).

The set of equations (2) can also be written in a matricial way:

$$\begin{pmatrix} \dot{x_0} \\ \dot{x_1} \\ \dot{x_2^1} \\ \vdots \\ \dot{x_2^n} \end{pmatrix} = \begin{pmatrix} f_0 Q & 0 & 0 & \cdots & 0 \\ f_0(1-Q) & f_1 Q' & 0 & \cdots & 0 \\ 0 & f_1(1-Q')q_1' & & & \\ \vdots & \vdots & & M_\mu D_{f_2} & \\ 0 & f_1(1-Q')q_n' & & & \end{pmatrix} \begin{pmatrix} x_0 \\ x_1 \\ x_2^1 \\ \vdots \\ x_2^n \end{pmatrix} - \Phi(\mathbf{x}) \begin{pmatrix} x_0 \\ x_1 \\ x_2^1 \\ \vdots \\ x_2^n \end{pmatrix},$$

where $M_\mu = \begin{pmatrix} \mu_{11} & \cdots & \mu_{1n} \\ \vdots & & \vdots \\ \mu_{n1} & \cdots & \mu_{nn} \end{pmatrix}$ and $D_{f_2} = \begin{pmatrix} f_2^1 & & \\ & \ddots & \\ & & f_2^n \end{pmatrix}$.

So, if we set M and D_f as the following matrices

$$M = \begin{pmatrix} Q & 0 & 0 & \cdots & 0 \\ 1-Q & Q' & 0 & \cdots & 0 \\ 0 & (1-Q')q_1' & & & \\ \vdots & \vdots & & M_\mu & \\ 0 & (1-Q')q_n' & & & \end{pmatrix}, \quad D_f = \begin{pmatrix} f_0 & & & & \\ & f_1 & & & \\ & & f_2^1 & & \\ & & & \ddots & \\ & & & & f_2^n \end{pmatrix},$$

then M is a Markov matrix by columns. This means that $\sum_{i=1}^{n+2} M_{ij} = 1 \, \forall j = 1 \div n+2$. This kind of matrix appears in mathematical models in biology (Usher 1971), economics [e.g., the Markov Switching Multifractal asset pricing model (Lux et al. 2011)], telephone networks [the Viterbi algorithm for error corrections (Forney 1973)] or "rankings" as the PageRank algorithm from Google (Sergey and Lawrence 1998; Bryan and Leise 2006). Therefore, the system can be rewritten as:

$$\dot{\mathbf{x}} = M D_f \mathbf{x} - \Phi(\mathbf{x})\mathbf{x}. \tag{2}$$

Our approach to this problem consists on assuming that $\{x_2^i\}$ behaves as an average variable $x_2 = \sum_{i=1}^{n} x_2^i$ (Solé and Deisboeck 2004). As a consequence, only two different mutation rates are involved in such simplified system: $\mu_0 = 1 - Q$ and $\mu_1 = 1 - Q'$. Hence, the set of equations is given by:

$$\begin{cases} \dot{x_0} = f_0 Q x_0 - \Phi(x_0, x_1, x_2)x_0, \\ \dot{x_1} = f_0(1-Q)x_0 + f_1 Q' x_1 - \Phi(x_0, x_1, x_2)x_1, \\ \dot{x_2} = f_1(1-Q')x_1 + f_2 x_2 - \Phi(x_0, x_1, x_2)x_2. \end{cases} \tag{3}$$

In this simplified system, the effect of mutations can be represented by means of a directed graph as shown in Fig. 1. From now on, let us assume that we always start with a population

entirely composed by stable cells, i.e., $x_0(0) = 1$ and $x_1(0) = x_2(0) = 0$. Notice that for this particular case every point of the trajectory always verifies $x_0 + x_1 + x_2 = 1$.

The model by Solé and Deisboeck (2004) considered $f_2 = \alpha f_1 \phi(\mu_1)$, where $\phi(\mu_1)$ was a decreasing function such that $\phi(0) = 1$, indicating that the speed of fitness decays as mutation increases, and where α was a competition term. The dependence of f_2 on f_1, μ_1, and α was introduced to take into account the deleterious effects of high genetic instability on the fitness of the unstable population x_2. In our work, we will consider f_2 as a constant, being independent of f_1 and μ_1. This assumption allows the analysis of a more general scenario where population x_1 can produce x_2 by mutation, and where x_2 can have different fitness properties depending on the selected values of both f_1 and f_2. For instance, we can analyze the case of deleterious mutations from x_1 to x_2 with $f_2 < f_1$. Such a case introduces in our system the deleterious effect of genomic instability, since mutations in compartment x_1 produce lower fitness mutants ($f_2 < f_1$) due to large number of mutations or chromosomal aberrations, typically found in tumor cells (Anderson et al. 2001). As a difference from the original approach followed by Solé and Deisboeck (2004), the deleterious effects of genomic instability in our analyses are implicitly included. The case of neutral mutations from x_1 to x_2 takes place when $f_2 = f_1$. Finally, the case of increased replication of x_2 populations is considered with $f_2 > f_1$. This latter case would correspond to mutations in driver genes that might confer a selective advantage to the tumor populations x_2.

3 Results and discussion

3.1 Equilibrium points

The system (3) has three different fixed points. Namely, a first one showing the total dominance of the unstable population, i.e., x_0 and x_1 go extinct and then $x_2 = 1$. A second one where x_0 goes extinct and x_1 coexists with x_2, and a third possible fixed point, where the three populations coexist. We cannot consider a fixed point with $x_0 \neq 0$, $x_2 \neq 0$ and $x_1 = 0$ because, as shown in Fig. 1, cells only mutate in one direction and it is not possible to have such scenario. Furthermore, the trivial equilibrium $x_0 = x_1 = x_2 = 0$ is never achieved because $x_0 + x_1 + x_2 = 1$.

Let us seek for these three possible fixed points. Then, we have to find the solutions of the following system:

$$\begin{pmatrix} 0 \\ 0 \\ 0 \end{pmatrix} = \begin{pmatrix} f_0 Q & 0 & 0 \\ f_0(1-Q) & f_1 Q' & 0 \\ 0 & f_1(1-Q') & f_2 \end{pmatrix} \begin{pmatrix} x_0 \\ x_1 \\ x_2 \end{pmatrix} - \Phi(\mathbf{x}) \begin{pmatrix} x_0 \\ x_1 \\ x_2 \end{pmatrix}. \tag{4}$$

- If we consider $x_0 = x_1 = 0$ and $x_2 \neq 0$, from the system (4) we obtain $f_2 x_2 - \Phi(x_0, x_1, x_2) x_2 = 0$, which has two possible solutions $x_2 = 0$ or $x_2 = 1$. As we require the sum of the three variables to be 1, then the solution is $(x_0^*, x_1^*, x_2^*) = (0, 0, 1)$.
- Let us consider now $x_0 = 0$ and then solve the obtained system of equations:

$$\begin{cases} f_1 Q' - f_1 x_1 - f_2 x_2 = 0, \\ f_1(1-Q')x_1 + f_2 x_2 - f_1 x_1 x_2 - f_2 x_2^2 = 0. \end{cases}$$

  Its solution is $x_1^* = \frac{f_1 Q' - f_2}{f_1 - f_2}$ and $x_2^* = \frac{f_1 - f_1 Q'}{f_1 - f_2}$. Notice that, as x_1 and x_2 are ratios of population, x_1^* and x_2^* must take values from 0 to 1. Then, from their expressions and remembering that $0 < Q' < 1$, we get the conditions: $f_1 > f_2$ and $f_1 Q' > f_2$.

- Finally, for the last fixed point, we consider $x_0 \neq 0, x_1 \neq 0, x_2 \neq 0$. Then, from the first equation of the system, we have $\Phi(x_0, x_1, x_2) = f_0 Q$. Hence, the new system has this form:

$$\begin{cases} f_0(1-Q)x_0 + (f_1 Q' - f_0 Q)x_1 = 0, \\ f_1(1-Q')x_1 + (f_2 - f_0 Q)x_2 = 0, \end{cases}$$

under the constraint $x_0 + x_1 + x_2 = 1$. Then, its solution is as follows:

$$x_0^* = \frac{(f_0 Q - f_1 Q')(f_0 Q - f_2)}{\varphi(f_0, f_1, f_2, Q, Q')},$$

$$x_1^* = \frac{f_0(1-Q)(f_0 Q - f_2)}{\varphi(f_0, f_1, f_2, Q, Q')},$$

and

$$x_2^* = \frac{f_1(1-Q')f_0(1-Q)}{\varphi(f_0, f_1, f_2, Q, Q')},$$

where

$$\begin{aligned} \varphi(f_0, f_1, f_2, Q, Q') = {} & (f_0 Q - f_1 Q')(f_0 Q - f_2) + f_0(1-Q)(f_0 Q - f_2) \\ & + (f_1(1-Q')f_0(1-Q). \end{aligned}$$

Remark 3.1 We can consider $f_1 = f_2$ as particular case. If these two fitness parameters are equal, the system (3) only has two possible fixed points. As we previously mentioned, this case would correspond to the production of neutral mutants from population x_1 to x_2.

From now on, we provide numerical results[1] of the system (3). To compute the solutions of this system, we have used the Taylor software. Taylor is an ODE solver generator that reads a system of ODEs and it outputs an ANSI C routine that performs a single step of the numerical integration of the ODEs using the Taylor method. Each step of integration chooses the step and the order in an adaptive way trying to keep the local error below a given threshold, and to minimize the global computational effort (Jorba and Zou 2004).

Numerically, we integrate the solution of system (3) with initial condition $(1, 0, 0)$. The next Lemma ensures that any point of this orbit satisfies $x_0 + x_1 + x_2 = 1$. It is used as an accuracy control while integrating the ODE system.

Lemma 3.1 *$S = x_0 + x_1 + x_2$ is a first integral of system (3), that is* $\dfrac{\mathrm{d}S}{\mathrm{d}t} = 0$.

Proof From the Eq. (3), we know that

$$\begin{aligned} \frac{\mathrm{d}S}{\mathrm{d}t} &= \dot{x_0} + \dot{x_1} + \dot{x_2} \\ &= f_0 Q x_0 + f_0(1-Q)x_0 + f_1 Q' x_1 + f_1(1-Q')x_1 + f_2 x_2 - \Phi(x_0 + x_1 + x_2) \\ &= \Phi(x_0, x_1, x_2)\,(1 - (x_0 + x_1 + x_2))\,. \end{aligned}$$

Since the initial condition is $x_0(0) = 1$ and $x_1(0) = x_2(0) = 0$, $1 - (x_0 + x_1 + x_2) = 0$ and the assertion follows. □

As a particular case, we consider $Q = 0.7$, $Q' = 0.3$ and $f_2 = 0.42$. Then, we make f_0 to take values from 0.01 to $\frac{1}{Q}$ and f_1 to take values from 0.01 to $\frac{1}{Q'}$ both with a step of 0.01.

[1] The codes used to obtain the results presented in this work are available upon request.

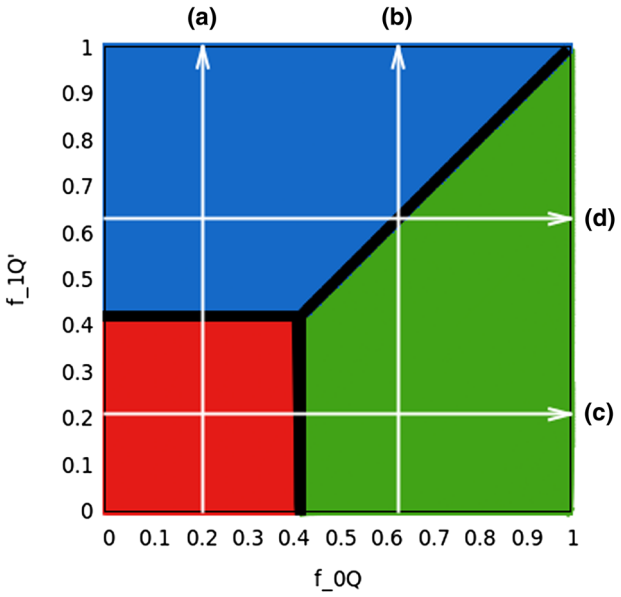

Fig. 2 Analysis of the parameter space $(f_0 Q, f_1 Q')$ to find the fixed points. Each *colored region* indicates a different fixed point [*smaller red square*: (0, 0, 1), with complete dominance of tumor cells x_2; *blue upper region*: $(0, x_1^*, x_2^*)$, with extinction of genetically stable cells and dominance of tumor cells; and *green region* at the *right*: (x_0^*, x_1^*, x_2^*), with coexistence of genetically stable and genetically unstable cells]. The *thick black lines* indicate that the system does not reach any fixed point. The *white arrows* are different sections that are studied along this work

We cannot start with $f_0 = 0$ or $f_1 = 0$ because this way x_0 or x_1 would become extinct. So, we compute the analytical result for all the possible fixed points and, with the iterative method, we integrate the ODE until the distance between the result of the iterate and one of the fixed points is less than an error tolerance previously set, in our case 10^{-16}. We also fix an upper limit for the time taken by the system to reach a preestablished distance to the fixed point, therefore we consider it does not reach any fixed point if this upper limit is surpassed.

These computations are displayed in Fig. 2, which shows the fixed points that are reached by the system depending on the parameters $f_0 Q$ and $f_1 Q'$. Here, each fixed point is indicated with a different colour. Red indicates that the fixed point is $x^* = (0, 0, 1)$; blue indicates that the fixed point is $x^* = \left(0, \frac{f_1 Q' - f_2}{f_1 - f_2}, \frac{f_1 - f_1 Q'}{f_1 - f_2}\right)$; and green indicates the fixed point where all subpopulations coexist. In addition, black lines indicate that none of the fixed points were reached by the system in the given time. Notice that in our analysis we are tuning $f_0 Q$ and $f_1 Q'$. The decrease of these pair of parameters is qualitatively equivalent to the increase of mutation rates μ_0 and μ_1, respectively, since $\mu_0 = 1 - Q$ and $\mu_1 = 1 - Q'$. For instance, going from $f_1 Q' = 1$ to $f_1 Q' = 0$ can be achieved increasing μ_1.

Figure 3 shows the density of each population at the equilibrium point in the same parameter space of Fig. 2. This analysis allows us to characterize the regions of this parameter space where the density of stable cells x_0 is high, and the malignant population x_2 remains low. As Solé and Deisboeck (2001) identified, this scenario can be achieved by increasing μ_1. Furthermore, our results suggest that this behavior is robust to changes in μ_0, whenever μ_0 remains small (i.e., high copying fidelity $f_0 Q$). Notice that an increase of $f_0 Q$ (or, alternatively, a decrease of μ_0) makes the population densities of x_0^* and x_2^* to increase and decrease, respectively, while for this range of parameters the values of x_1^* remain low. This

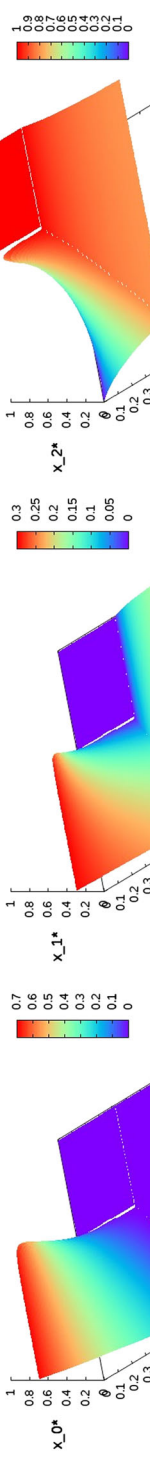

Fig. 3 Equilibrium concentration of each variable in the parameter space (f_0Q, f_1Q'). We display the equilibrium value for genetically stable cells, x_0 (*left panel*); and tumor cell populations x_1 (*middle panel*) and x_2 (*right panel*). Notice that the *color bar* for each panel is not normalized

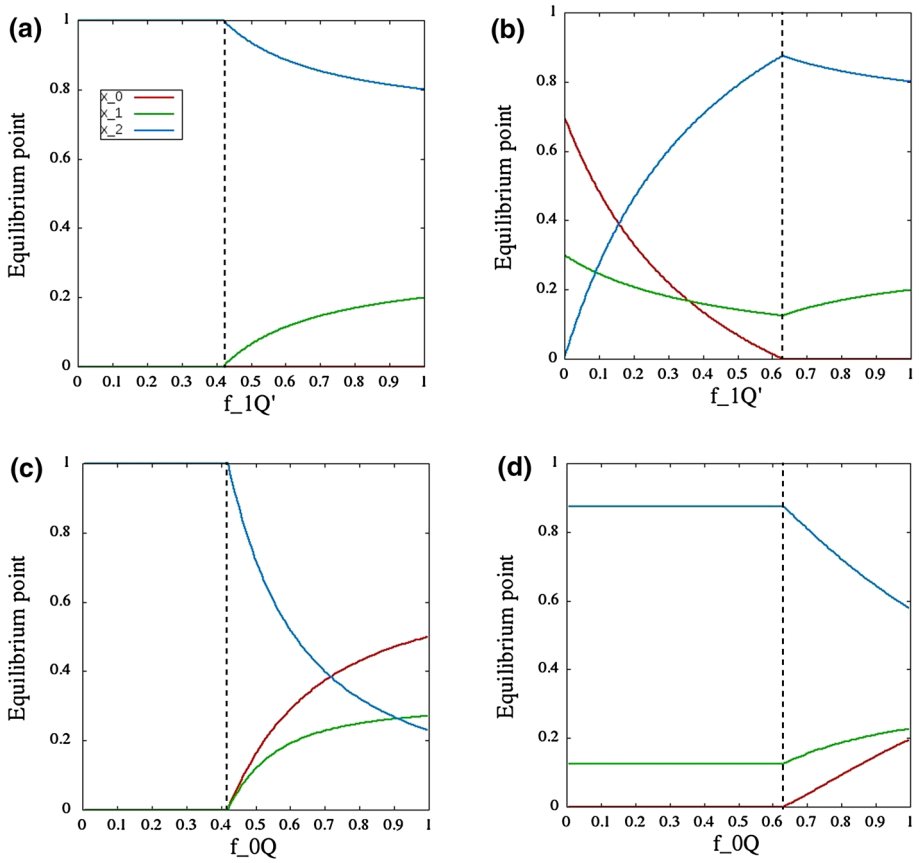

Fig. 4 Impact of changing the replication fidelity of the populations x_0 and x_1, i.e., $f_0 Q$ and $f_1 Q'$, respectively, in the equilibria of the three cell populations. In **a** and **b** $f_0 Q$, has fixed values 0.21 and 0.63, respectively; in **c** and **d**, f_1 has fixed values 0.21 and 0.63. Notice that the *letter of each panel* corresponds to sections made in Fig. 2, represented by the *white arrows*. *Vertical dashed lines* indicate the bifurcation values

highlights the relevance of targeted mutagenic therapies against tumor cells, while the most stable cells should keep replicating with a high fidelity. Such a therapy may slow down tumor growth, which could be eventually cleared due to demographic stochasticity because of the small population numbers for x_2 found for this combination of parameters (i.e., large μ_1 together with low μ_0).

We observe that there is a frontier between the different fixed points reached by the system. In this case, the shift from one fixed point to another is given by a bifurcation. In Fig. 4, we appreciate these bifurcations (see dashed vertical lines) more clearly (in the next section, we will study the bifurcations in detail). For this purpose, we have set four sections of Fig. 2 (white arrows), i.e., we have fixed different values for f_0 and f_1. In this case, these values are $f_0 Q = 0.21, 0.63$ and $f_1 Q' = 0.21, 0.63$.

We see the bifurcations of the fixed points of the system in Fig. 4. In (a) and (b), $f_0 Q$ has fixed values 0.21 and 0.63, respectively, so bifurcations are represented depending on the replication fidelity of x_1 in both cases. We notice that for high replication fidelity only x_1 and x_2 coexist. But in (b) the case is different: if we study this graphic in terms of the mutation rate of x_1 we can observe that for high values of it, the system stays at an equilibrium

point where x_0 is greater. That means that if we make the mutation rate μ_1 higher enough through therapy it is possible to make the tumor to achieve an equilibrium state where the most unstable cells are near to 0 and the whole population is mainly dominated by x_0.

In cases (c) and (d), we have considered fixed values $f_1 Q' = 0.21$ and $f_1 Q' = 0.63$ and, therefore, now bifurcations are represented in terms of the replication fidelity of x_0. Notice that in both cases the higher is the probability of x_0 to stay stable (equivalently, the mutation rate μ_0 of x_0 is low) the higher is the population of stable cells at the equilibrium point. This is crucial since they correspond to final scenarios with an important presence of genetically stable cells. Comparing these cases, we observe that, if the mutation rate of x_1 is higher, i.e., case (c) ($f_1 Q' = 0.21$, i.e., $f_1 \mu_1 = 0.49$), the population x_0 in the equilibrium point reached is also higher. This suggests the existence of a threshold in the unstability of x_1 bringing more stable cells x_0 into the final equilibria.

3.2 Stability analysis and bifurcations

The linear stability analysis of the fixed points characterized in the previous section is performed using the Jacobi matrix:

$$L_\mu(x^*) = \begin{pmatrix} f_0 Q - \Phi(\mathbf{x}) - x_0 f_0 & -x_0 f_1 & -x_0 f_2 \\ f_0(1-Q) - x_1 f_0 & f_1 Q' - \Phi(\mathbf{x}) - x_1 f_1 & -x_1 f_2 \\ -x_2 f_0 & f_1(1-Q') - x_2 f_1 & f_2 - \Phi(\mathbf{x}) - x_2 f_2 \end{pmatrix}.$$

We are specially concerned with the domain, in the parameter space, where the malignant cells become dominant, and the stability of such equilibrium state. Thus, taking $x^* = (0, 0, 1)$, the Jacobi matrix has the following eigenvalues:

$$\lambda_1 = f_0 Q - f_2, \lambda_2 = f_1 Q' - f_2, \quad \text{and} \quad \lambda_3 = -f_2.$$

So, x^* is an attractor if the two inequalities, $f_0 Q < f_2$ and $f_1 Q' < f_2$, are satisfied. From the expression of the eigenvalues, we conclude that there is a critical condition for the mutation rates $\mu_0 = 1 - Q$ and $\mu_1 = 1 - Q'$, given by: $\mu_0^c = 1 - \frac{f_2}{f_0}$ and $\mu_1^c = \frac{f_2}{f_1}$, respectively [see also (Solé and Deisboeck 2004)].

These conditions separate the domain where only x_2 remains from the other two cases. From Fig. 5a we can confirm that the fixed point $x^* = (0, 0, 1)$ is an attractor point until this critical condition i.e., the error threshold, (shown by a vertical dotted line) is reached. From that value, the fixed point x^* is unstable, with local 2-dimensional stable invariant manifold and a 1-dimensional unstable one.

If we evaluate the stability of the fixed point $x^* = \left(0, \frac{f_1 Q' - f_2}{f_1 - f_2}, \frac{f_1 - f_1 Q'}{f_1 - f_2}\right)$, where populations x_1 and x_2 coexist, we get the following eigenvalues from the Jacobi matrix:

$$\lambda_1 = f_0 Q - f_1 Q', \lambda_2 = \frac{f_1(f_2 - f_1 Q')}{f_1 - f_2}, \quad \text{and} \quad \lambda_3 = \frac{2 f_1 f_2 Q' - f_1^2 Q' - f_2^2}{f_1 - f_2}.$$

Observe that from the condition of fixed point it follows that $f_2 < f_1 Q'$ so, therefore, $\lambda_2 < 0$ and $\lambda_3 = -\frac{1}{f_1 - f_2}\left((f_1 Q' - f_2)^2 + f_1^2 Q'(1 - Q')\right) < 0$. This means that its linear stability depends on the sign of $\lambda_1 = f_0 Q - f_1 Q'$.

Notice that, as we mention in Remark 3.1, when $f_1 = f_2$, such fixed point does not exist, hence the eigenvalues of the Jacobi matrix do not provide any information. This can be appreciated in Fig. 5b, when $f_1 Q' = 0.126$, thus $f_1 = f_2 = 0.42$.

Finally, we want to study the stability of the fixed point where all populations coexist. An analytical expression for the eigenvalues exists, since we have the Jacobi matrix and the

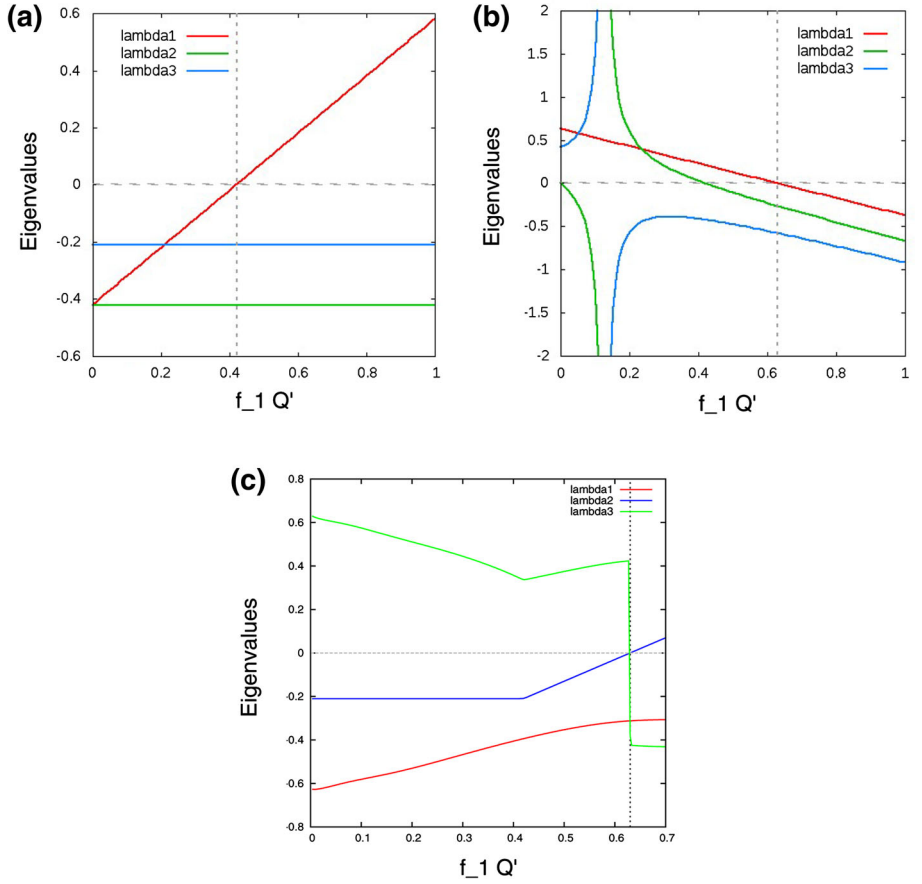

Fig. 5 **a** Eigenvalues of $L_\mu(x^*)$ for $x^* = (0, 0, 1)$ and $f_0 Q = 0.21$, using the range of the *arrow* (**a**) in Fig. 2. **b** Eigenvalues of $L_\mu(x^*)$ as a function of $f_1 Q'$ for the fixed point $x^* = (0, x_1^*, x_2^*)$ using $f_0 Q = 0.63$. **c** Eigenvalues of the differential at the equilibrium point as a function of $f_1 Q'$. The *vertical dotted line* indicates the bifurcation value at $f_1 Q' = 0.63$.

analytical expression for the fixed point itself. But they have really complicated expressions and, even more, we are considering $n = 1$. This means that the greater n, the analytical expressions for the eigenvalues are more complicated to find. This is the reason why it is interesting to compute them numerically.

To compute the eigenvalues of this three-dimensional matrix, we proceed in the following way. This simplified procedure turns to be quite fast in our case (dimension 3) but may not be applicable for higher dimensions. It works as follows:

- We first apply the power method to compute an approximation for the eigenvalue of maximal modulus. As it is known, it is based on the idea that the sequence $v_{k+1} = Av_k$ should behave for large values of k as the direction of the eigenvector associated to the largest (in modulus) eigenvalue $\lambda_{\max}$ of A. To compute it one starts from an arbitrary initial vector v_0 (in our case, for instance, $(1/3, 1/3, 1/3)$, and computes $v_{k+1} = Av_k$. Provided the difference between the largest eigenvalue and the second largest eigenvalue (in modulus, always) is not too small, the quotients of the components of v_{k+1}, v_k, that

is $v_{k+1}^{(j+1)}/v_{k+1}^{(j)}$, converge to $\lambda_{\max}$. To avoid problems of overflow, one normalizes v_{k+1}, i.e. $w_{k+1} = v_{k+1}/\parallel v_{k+1} \parallel$, at any step. Problems of convergence appear when the two largest eigenvalues of A are close.

- We apply the same method to A^{-1} to obtain the smallest eigenvalue of A, since λ is eigenvalue of A iff λ^{-1} is eigenvalue of A^{-1}. To compute A^{-1}, we have used its QR-decomposition, which writes A as the product of two matrices: an orthogonal matrix Q and an upper triangular matrix R, i.e., $A = QR$.
- Provided $\lambda_{\max}$, $\lambda_{\min}$ are accurate enough, the third eigenvalue is determined from the value of the determinant of the matrix A, that we have derived from its QR-decomposition.

We apply this procedure to the study of possible bifurcations in the stability of the equilibrium points obtained when we do not have analytic expressions for the associated eigenvalues. To show it, we fix a value for $f_0 Q$ and move $f_1 Q'$. We have chosen a value for $f_0 Q$ corresponding to the line (b)of the diagram in Fig 2. Observe that, when moving at the green zone our equilibrium point is of the form $(x_0^*, x_1^*, 1-x_0^*-x_1^*)$ while it is of the form $(0, x_1^*, 1-x_1^*)$ when we move along the blue one. For each equilibrium point, whose components depend on $f_1 Q'$, we compute its differential matrix and its associated eigenvalues. These eigenvalues, computed numerically as mentioned above, are plotted in Fig. 5c. They are all three real, and thus no transient oscillations are found in the dynamics. Observe that there is an interchange of the number of positive and negative eigenvalues around the bifurcation value 0.63, but no change in their stability. They are always unstable since we have at least one positive eigenvalue.

The model by Solé and Deisboeck, which considered the deleterious effects of genomic instability explicitly, identified that increased μ_1 (or decreased Q') involved the transition from dominance of x_2 populations to dominance of healthy cells and impairment of most unstable cells x_1 and x_2. We also identified such phenomenon (see Figs. 2, 3, 4, 5), characterizing the existence of a transcritical bifurcation governing such transition. This finding suggests that the same type of bifurcation may be found in the original model which considered the functional relation $f_2 = \alpha f_1 \phi(\mu_1)$. In our particular system, it is interesting to highlight the change in the geometry of the equilibrium point $(x_0^*, x_1^*, 1-x_0^*-x_1^*)$: for values of $f_1 Q'$ under the bifurcation value 0.63, its invariant stable manifold is two dimensional and its invariant unstable manifold one dimensional; on the contrary, after the bifurcation the associated dimensions of the invariant manifolds are exchanged. In both cases, the orbit starting at initial conditions $(1, 0, 0)$ finishes at the stable manifold of that equilibrium point. This is why, although being a unstable fixed point, the trajectory under analysis asymptotically travels towards the fixed point.

3.3 Transient times

In this section, we analyze the time taken by the system to reach a given (small) distance to one of the fixed points found in Sect. 3.1. Typically, the behavior of transient times changes near bifurcation threshold, and, particularly for our system, we are interested in possible changes in transients due to changes in mutation rates. These phenomena could be relevant in patient response under mutagenic therapy.

Figure 7 shows the same as Fig. 2, in the sense that we tune the same parameters of the system, but now we compute the transient times. Here, we use the same method to integrate the ODE system, but taking into account only the time taken to reach a distance 10^{-2} of the equilibrium point. Notice that if we observe the contour lines represented at the bottom of

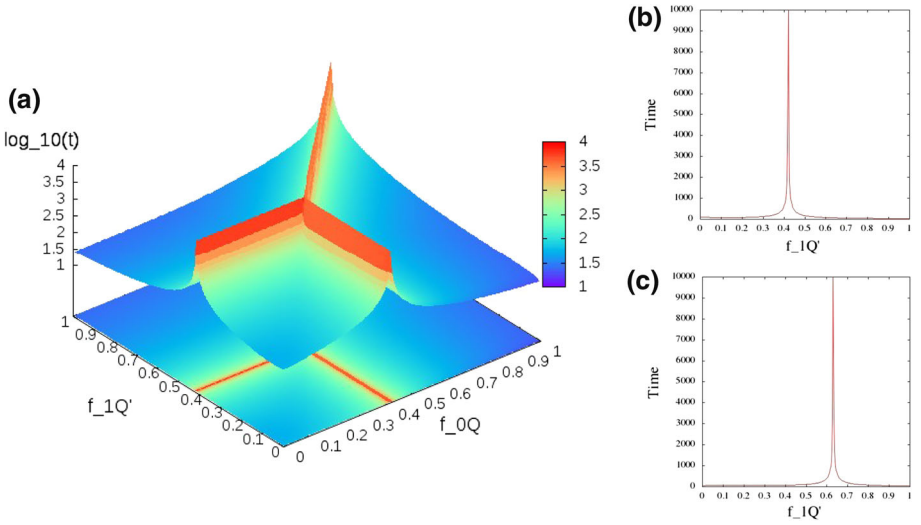

Fig. 6 Time taken by the system to reach a distance 10^{-2} to a fixed point in the parameter space $(f_0 Q, f_1 Q')$. Time in **a** is logarithmic represented in base 10 but in sections **b** and **c** it is represented in real scale due to appreciate the actual velocity of the system and its sharp change near bifurcation threshold

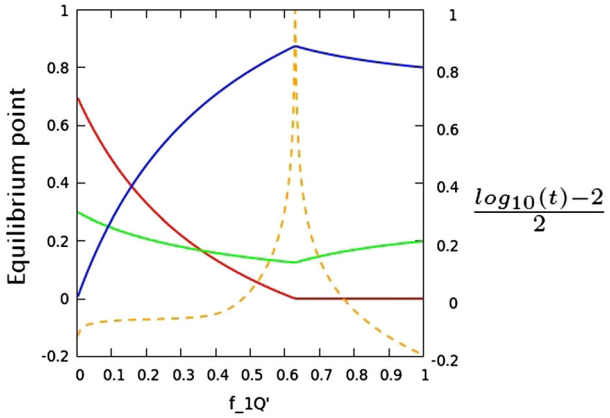

Fig. 7 Transient times dependence on $f_1 Q'$. *Dashed line* $\frac{\log_{10}(t)-2}{2}$, and the *solid lines* are the equilibrium densities of genetically stable cells, x_0 (*red*); and tumor cells x_1 (*green*) and x_2 (*blue*) for $f_0 Q = 0.63$. Notice that time is maximum at the bifurcation value

Fig. 6 we have the same as in Fig. 2. This means that the "time to equilibrium" of the system increases when we are near bifurcation points, which are represented with black lines in Fig. 2.

When slightly modifying the mutation rate of x_1 near the error threshold, we see that the time taken by the tumor to reach an equilibrium state is significantly lower. In particular, when increasing the mutation rate, not only time decreases but also we see that the tumor reaches an equilibrium point where the stable cells population is higher. This can be appreciated in Fig. 7, where red, green and blue lines represent x_0, x_1 and x_2, respectively, and the dashed, orange line represents the transient time, which is rescaled to be able to relate it with the corresponding equilibrium point. In case of possible mutagenic therapies directly targeting the most unstable cells, our results reveal that pushing mutation rates of unstable

cells beyond the error threshold (where x_0 population starts increasing and x_2 population starts decreasing) the achievement of the equilibrium point would be very fast, and no further increase of mutation rates may be needed to achieve a faster response (notice that the transient time for $f_1 Q' \lessapprox 0.45$ in Fig. 6 does not significantly decrease for smaller $f_1 Q'$ values). In other words, when rescaling Fig. 6b in terms of logarithm in base 10 (as we can see in Fig. 7) if we increase the mutation rate of x_1, time decreases faster than an exponential function, which is interesting result since it implies an equilibrium scenario with a dominant presence of x_0 that can be reached in a short time.

4 Conclusions

In this article, we study an ODE system modeling the competition dynamics between genetically stable and tumor cells with different levels of genomic instability with a mean-field quasispecies model introduced by Solé and Deisboeck (2004). This model does not consider stochasticity and does not take into account spatial correlations between cells as well. Also, no cell death is introduced (due to e.g., the immune system), otherwise the model introduces competition in terms of replication and mutation using the quasispecies framework (Eigen 1971; Eigen and Schuster 1979).

First, we have found the fixed points of the system analytically and we have studied their stability both analytically and numerically. We have also characterized the bifurcations between the different fixed points in terms of their replication fidelities $f_0 Q$ and $f_1 Q'$. We conclude that, depending on the parameters, the system can reach three different equilibrium states, one of them involving low populations of tumor cells while keeping large populations of genetically stable cells. This scenario can be achieved by increasing the mutation rate μ_1 of the mutator phenotype population x_1, together with large values of $f_0 Q$ (see e.g., the most right panel in Figs. 3, 4c). It is known that tumor cells usually increase proliferation rates due to mutations in tumor suppressor genes or oncogenes. Such mutations are named driver mutations since they confer a selective advantage in terms of competition. In this sense, it might be biologically plausible that the replication rate of x_1 populations might be larger than the replication of genetically stable cells (i.e., $f_1 > f_0$). That would place the system to the regime of extinction of x_0 populations (see Fig. 2). However, one might expect the product $f_0 Q$ to be large since the copying fidelity of x_0 populations is extremely large compared to the copying fidelity of most unstable tumor populations. Normal cells display a very low rate of mutation (1.4×10^{-10} changes per nucleotide and replication cycle), while it has been shown in both experimental and clinical cases, that mutations that inactivate mismatch repair genes result in $10^2 - 10^3$ times the background mutation rate (Oliver et al. 2000; Bjedov et al. 2003; Sniegowski et al. 1997). According to this fact, the case where populations coexist with dominance of x_0 populations may be naturally found. This scenario was also found in the original model of Ref. Solé and Deisboeck (2004) which explicitly considered the deleterious effects of increased genomic instability of tumor cells. In agreement with the approach followed in Ref. Solé and Deisboeck (2004), we also found that if mutation rate μ_1 exceeds an error threshold, the replication rate of the more malignant subpopulation x_2 is reduced to a point where it has no longer competitive advantage.

Linear stability analyses have allowed us to characterize a transcritical bifurcation at increasing mutation rate μ_1 (or decreasing Q'). Transient time responses after mutagenic therapy are extremely important to quantify the time needed for the system to achieve the desired equilibrium state: in this case, dominance of x_0 and lower population values of $x_{1,2}$. Under such a bifurcation, the time taken by the system to reach this equilibrium state is shown

to diverge as we approach to the bifurcation point. We notice that such a phenomenon is local i.e., a slight increase of the mutation rate μ_1 above the error threshold largely decreases the time to achieve the fixed point (Figs. 6, 7). This result can give us a clue about how medication and therapy may affect the tumor behavior in case of specific mutagenic therapies against tumor cells. In this sense, the so-called targeted cancer therapies could be used to deliver mutagenic drugs to cancer cells. For instance, a bioinspired cocoon-like anticancer drug delivery system composed of a DNase-degradable DNA nano clew embedded in a DNase I nano capsule has been recently developed to target and deliver drugs specifically inside cancer cells (Sun et al. 2014). Roughly, such nano capsules self-degrade in the presence of low pH (acidic conditions), found in the lysosomes when they are internalized in the tumor cells in a selective manner via folate receptors, releasing the drug able to act inside the nucleus of tumor cells. For this particular case, the cocoon-like self-degradation released the anticancer drug DOX (doxorubicin) inside the tumor cells (Sun et al. 2014). DOX acts on macromolecular synthesis, inhibiting the progression of the enzyme topoisomerase II during DNA replication. One effect of such inhibition is the increase of free radical production within targeted cancer cells, which could involve increased mutagenesis in such cells. In this sense, it is known that oxidative damage can increase the mutation frequency by an average 4.3-fold (Feig and Loeb 1993). Extensively, other mutagenic drugs such as base analogs or intercalating agents could be applied to cancer cells by means of the cocoon-like nano capsules.

Since it may be possible to increase mutations in tumor cells through targeted cancer therapy, the mutation frequency could be probably driven beyond the critical mutation rate of x_1. Then, according to the simple model analyzed in this article, the system would reach an equilibrium point with a dominant population of stable cells rapidly. Such an scenario could become relevant since populations of tumor cells could be decreased with this type of therapy, being more prone to extinction due to stochastic fluctuations inherent to small population sizes or due to the action of the immune system.

Further research should explicitly consider stochastic fluctuations by transforming the differential equations in stochastic differential equations e.g., Langevin equations. Also, the addition of spatial correlations would indicate if our results are still present in theoretical models for solid tumors. In this sense, it would be interesting to analyze the transient times tied to increasing mutation values considering space in an explicit manner. As mentioned, transient times are extremely important in terms of response velocities after therapy. Different causes and mechanisms have been suggested to be involved in transient duration, which have been especially explored for ecological systems (Hastings 2004). For instance, it is known that space can involve very long transients until equilibrium points are reached. This phenomenon could be investigated extending the model we investigated by means of partial differential equations.

Acknowledgments We want to thank Ricard V. Solé for helpful comments and suggestions. JTL has been partially supported by the Spanish MICIN/FEDER grant MTM2012-31714, by the Generalitat de Catalunya grant number 2014SGR-504, and by grant 14-41-00044 of RSF at the Lobachevsky University of Nizhny Novgorod. JS has been funded by the Fundación Botín.

References

Anderson GR, Stoler DL, Brenner BM (2001) Cancer as an evolutionary consequence of a destabilized genome. Bioessays 23:103746

Benedikt B, Siebert R, Traulsen A (2014) Cancer initiation with epistatic interaction between driver and passenger mutations. J Theor Biol 358:52–60

Bielas JH, Loeb KR, Rubin BP, True LD et al (2006) Human cancers express a mutator phenotype. Proc Natl Acad Sci 103:18238–18242
Bjedov I, Tenaillon O, Gérard B, Souza V et al (2003) Stress-induced mutagenesis in bacteria. Science 300(14049):35
Brumer Y, Michor F, Shakhnovich EI (2006) Genetic instability and the quasispecies model. J Theor Biol 241:216–222
Bryan K, Leise T (2006) The $25,000,000,000 eigenvector. The linear algebra behind Google. SIAM Rev 48(3):569–581
Bull JJ, Sanjuán R, Wilke CO (2007) Theory of lethal mutagenesis for viruses. J Virol 81:2930–2939
Cahill DP, Kinzler KW, Vogelstein B, Lengauer C (1999) Genetic instability and darwinian selection in tumors. Trends Genet 15:M57–M61
Cairns J (1975) Mutation selection and the natural history of cancer. Nature 255:197–200
Cichutek K, Merget H, Norlay S, Linde R et al (1992) Development of a quasispecies of human immunodeficiency virus type 1 in vivo. Proc Natl Acad Sci 89:7365–7369
Crotty S, Cameron CE, Andino R (2001) RNA virus error catastrophe: direct molecular test by using ribavirin. Proc Natl Acad Sci 98:6895–6900
Domingo E, Biebricher CK, Eigen M, Holland JJ (2001) Quasispecies and RNA virus evolution: principles and consequences. Landes Bioscience, Georgetown
Eigen M (1971) Selforganization of matter and evolution of biological macromolecules. Naturwissenschaften 58:465–523
Eigen M, Schuster P (1979) The hypercycle: a principle of natural selforganization (Springer-Verlag New York). Naturwissenschaften 58:465–523
Feig DI, Loeb LA (1993) Mechanisms of mutation by oxidative DNA damage: reduced fidelity of mammalian DNA polymerase β. Biochemistry 32:4466–4473
Forney GD (1973) The Viterbi algorithm. Proc IEEE 61:268–278
Hastings A (2004) Transients: the key long-term ecological understanding. Trends Ecol Evol 19:39–45
Hoeijmakers JH (2001) Genome maintenance mechanisms for preventing cancer. Nature 411:366–374
Jorba Á, Zou M (2004) A software package for the numerical integration of ODEs by means of high-order Taylor methods. http://www.maia.ub.es/angel/taylor/taylor.pdf
Lauring AS, Andino R (2010) Quasispecies theory and the behavior of RNA viruses. PLoS Pathog 6(7):e1001005
Loeb LA (2001) A mutator phenotype in cancer. Cancer Res 61:3230–3239
Lux T, Morales-Arias L, Sattarhoff C (2011) A Markov-switching multifractal approach to forecasting volatility. Kiel Working Paper, 1737
Marcus PI, Rodriguez LL, Sekellick MJ (1998) Interferon induction as a quasispecies marker of Vesicular stomatitis virus populations. J Virol 72(1):542–549
Merlo LMF, Pepper JW, Reid BJ, Maley CC (2006) Cancer as an evolutionary and ecological process. Nat Rev Cancer 6:924–935
Nowak MA (1992) What is a quasispecies? Trends Ecol Evol 7:118–121
Oliver A, Canton R, Campo P, Baquero F et al (2000) High frequency of hypermutable *Pseudomonas aeruginosa* in cystic fibrosis lung infection. Science 288:12514
Sardanyés J, Simó C, Martínez R, Solé RV, Elena SF (2014) Variability in mutational fitness effects prevents full lethal transitions in large quasispecies populations. Nat Sci Rep 4:4625
Sergey B, Lawrence P (1998) The anatomy of a large-scale hypertextual web search engine. Comput Netw ISDN Syst 33:107–117
Sniegowski PD, Gerrish PJ, Lenski RE (1997) Evolution of high mutation rates in experimental populations of *E. coli*. Nature 387:7035
Solé RV (2001) Phase transitions in unstable cancer cells populations. Eur Phys J B 35:117–123
Solé RV, Sardanyés J, Díez J, Mas A (2006) Information catastrophe in RNA viruses through replication thresholds. J Theor Biol 240:353–359
Solé RV, Deisboeck TS (2004) An error catastrophe in cancer? J Theor Biol 228:47–54
Sun W, Jiang T, Lu Y, Reiff M, Mo R, Gu Z (2014) Cocoon-like self-degradable DNA nano clew for anticancer drug delivery. J Am Chem Soc 136:14722–14725
Swetina J, Schuster P (1982) Self-replication with errors. A model for polynucleotide replication. Biophys Chem 16:329–345
Usher MB (1971) Developments in the Leslie model in mathematical models in ecology. Blackwell Scientific Publications
Wylie CS, Shakhnovich EI (2012) Mutation induced extinction in finite populations: lethal mutagenesis and lethal isolation. PLoS Comput Biol 8(8):e1002609